Research Article | Vol. 29, No. 17 / 16 Aug 2021 / Optics Express 27807

Optics EXPRESS

Bose-Einstein condensation of photons in a long fiber cavity

RAFI WEILL, ALEXANDER BEKKER, BORIS LEVIT, AND BARUCH FISCHER*

Andrew and Erna Viterbi Faculty of Electrical Engineering, Technion, Haifa 32000, Israel
**fischer@ee.technion.ac.il*

Abstract: We demonstrate photon Bose-Einstein condensation (photon-BEC) at a broad temperature range that is valid also in the long 1D fiber cavity limit. It is done with an erbium-ytterbium co-doped fiber (EYDF) cavity by overcoming the challenging requirement of sublinear light dispersion for BEC in 1D using a chirped-gratings Fabry-Perot. We experimentally show with a square-root mode-dispersion, a quadratic temperature dependence of the critical power for condensation (compared to a linear dependence in finite regular fiber-cavities) between 90 K and 382 K, as the theory predicts.

1. Introduction

Bose-Einstein Condensation (BEC) was predicted in 1924-5, but it took 70 years to experimentally observe it with atomic bosons at ultra-low temperatures [1,2]. More recently it was observed with non-atomic bosons such as photons [3,4], exciton-polaritons and magnons [5–8]. Photon-BEC has been observed so far only in two systems at close to room temperatures but with limitations: in a two-dimensional (2D) dye-filled microcavity [3] and in a one-dimensional (1D) erbium-ytterbium co-doped fiber cavity [4] . BEC is characterized by a transition to a macroscopic population of bosons at the ground state at a nonzero temperature. It generally depends on the dimension, the dispersion relation that for light is commonly linear (exponent of 1), and the sort of a possible potential trap [9]. A dispersion with an exponent of 1 is at the boundary for BEC in one-dimension (1D) without a potential trap that requires exponents smaller than 1 [4,9]. It makes the integral for the bosonic particles converge (see below Eq. (4) and the discussion there) meaning that all states above the ground state are filled at some stage (critical temperature or critical particle number) and any additional pumping (or decrease of the temperature) adds particles to the ground state. In the fiber photon-BEC case the condensation observation was possible only due to a finite system size [4,10]. In the dye-filled microcavity [3,11–13]. BEC was observed with the transverse cavity modes that provided a two-dimensional (2D) system with a quadratic dispersion (exponent of 2) for the transversal wave-vector components. A dispersion exponent of 2 is again on the boundary for BEC in 2D and it therefore needed a potential trap that was provided by the broad cavity mirrors [3,11–13]. Thermalization and condensation were recently observed also in an electrically pumped semiconducor microresonator [14].

In the present work, we overcome a crucial requirement for photon-condensation in 1D fibers without a potential-trap by using a special sublinear mode-dispersion technique that makes the condensation valid also in the large system limit, without the need of a finite cavity dependent condensation used in Ref. 4. The dispersion near a cutoff frequency $(\omega - \omega_0) = a(k - k_0)^\eta$ requires in 1D a sublinear positive exponent $(0<\eta<1)$ [4,5], which we achieved by a chirped fiber Bragg gratings Fabry-Perot (FP) [15]. For a linear chirp, the case of our experiments, the mode-dispersion has a square-root dependence on the FP mode number. The FP was placed in a fiber cavity with erbium-ytterbium co-doped double-clad fiber (EYDF) that provided the BEC requirements for photon thermalization [4,16], and together with the photon number conservation provided by gain [3,4,11], and a cutoff frequency that determined the ground state [4], we

#430406 https://doi.org/10.1364/OE.430406
Journal © 2021 Received 5 May 2021; revised 30 Jun 2021; accepted 26 Jul 2021; published 13 Aug 2021

Optics EXPRESS

obtained BEC. We studied such chirped fiber Bragg gratings FP in another paper [15], where we gave analytical calculation and experimental demonstration of sublinear mode-dispersion, and a density of mode states (DOS) with a positive nonzero exponent near a cutoff frequency, as required for BEC. We also demonstrate here the temperature dependence of the condensation threshold (critical) power that is found to be quadratic in a broad temperature range between 90 K and 382 K for a linear chirped gratings case that follows the theoretical prediction. This quadratic temperature dependence that results from the square-root mode-dispersion adds a support to the BEC observation. For comparison, we also show results of a linear temperature dependence of the condensation threshold power in a regular fiber cavity without the mode-dispersion modification of the chirped fiber Bragg gratings FP that relies on the finite size property. It is similar to the condensation that we obtained in Ref. [4]. We also mention former works on distinguishing between photon BEC and laser oscillation and other condensation phenomena, including classical (Rayleigh-Jeans) condensation of waves in lasers, nonlinear crystals and multimode fibers [17–25].

2. BEC in long cavities

As mentioned above BEC in 1D requires a sublinear dispersion near a cutoff frequency that gives there a nonzero DOS exponent. Therefore, before analyzing the condensation formation in our case, we give a short description on the experimental way to obtain such dispersion. We recently reported on that in the paper of Ref. [15].

2.1. Sublinear mode-dispersion by chirped gratings Fabry-Perot

The needed sublinear dispersion can be achieved by a FP with two chirped fiber Bragg gratings with opposite chirp directions. The Bragg wavelength changes along the grating according to: $z_1 = C^{-1}(\lambda_0 - \lambda)^\alpha$ and the close wavelength locations are at λ_0. C is the chirp strength that can be positive or negative according to the chirp direction. The chirp nonlinearity is given by the exponent α. The C dimension is $(meter)^{\alpha-1}$. In our experiment we had a linear chirp with $\alpha = 1$ and a dimensionless chirp strength $C = 2 \times 10^{-6}$. The high wavelength chirp edge is at λ_0 or $\omega_0 = 2\pi c/(n\lambda_0)$ that with the wave-shaper serve as the cutoff. The upper wavelength of the wave-shaper transmission band was prepared to be close and slightly below the wavelength of the grating's chirp edge. Therefore the effective distance between the gratings was here $l_0 = 2.8\,mm$, higher than the value in Ref. [15] with $l_0 = 0.3\,mm$, but still small to get the needed DOS for BEC. The FP effective length is $l_{eff} = 2z_1 + l_0 = 2C^{-1}(\lambda_0 - \lambda)^\alpha + l_0$, where l_0 is the spacing between the two chirped fiber Bragg gratings. We mostly want to have small l_0. We give here only the results [15], The density of light-mode states (DOS) of the chirped fiber Bragg gratings FP for $(\omega - \omega_0)/\omega_0 << 1$ (valid in our case in the whole band)**:**

$$\rho(\omega) \approx b(\omega - \omega_0)^\alpha + \rho_0\,, \tag{1}$$

where $\rho_0 = l_0/(\pi c/n)$ and $b = 4C^{-1}(2\pi c/n)^{\alpha-1}/{\omega_0}^{2\alpha}$.

For FP gratings with a linear chirp ($\alpha = 1$): $\rho(\omega) \approx b(\omega - \omega_0) + \rho_0$, where $b = 4C^{-1}/{\omega_0}^2$. Therefore, the DOS $\rho(\omega)$ increases with ω and the spacing between modes $\Delta\omega$ decreases until they both become constant since $((\omega - \omega_0)/\omega)^\alpha \to 1$ for $\omega >> \omega_0$. The mode-dispersion near the cutoff for the linear chirp case ($\alpha = 1$):

$$\begin{aligned}(\omega - \omega_0) &= [-\rho_0 + (\rho_0^2 + 2\,b\,m)^{1/2}]/b \\ (\lambda_0 - \lambda) &\approx [{\lambda_0}^2/(2\pi c/n)]\ [-\rho_0 + (\rho_0^2 + 2\,b\,m)^{1/2}]/b\end{aligned} \tag{2}$$

where $m = 0, 1, 2\ldots$ is the FP mode number. With $l_0 \approx 0$ ($\alpha = 1$) we have a square-root mode-dispersion [15]:

$$(\omega - \omega_0) = (2/b)^{1/2}\, m^{1/2}. \tag{3}$$

Optics EXPRESS

The general α case than can be mapped to a nonlinear dispersion $(\omega - \omega_0) = a\,(k - k_0)^{\eta}$ that gives for the FP modes DOS, $\rho(\varepsilon) \propto 1/(d\omega/dk) \propto \varepsilon^{(1/\eta)-1}$, where $\eta = 1/(\alpha+1)$ or $\alpha = (1/\eta)-1$. The linear case ($\alpha = 1$) corresponds to a square-root dispersion $(\omega-\omega_0) = a\,(k - k_0)^{1/2}$ ($\eta = 1/2$).

2.2. Photon-BEC temperature dependence

We first mention discussions on which ensemble, grand-canonical, canonical or microcanonical, should be used for BEC [26]. Most analyses were done with a grand-canonical ensemble where the system is in a thermal and chemical equilibrium with a reservoir, exchanging energy and particles, compared to a fix particle number in a canonical ensemble, as is the case in many experiments. In our case of photon BEC only the average power or the average photon number, and not the number itself, are kept constant by the pumping [3,4]. The average occupations are the same in the abovè ensembles, but the fluctuations at the condensation state in the grand-canonical ensemble are large, on the order of the particle number N [26]. In the grand-canonical ensemble the average number of photon particles is $N = \sum_{\omega_i \geq \omega_0} 1/\{\exp\beta[\hbar(\omega_i - \omega_0) - \mu] - 1\}$, where ω_i are the states (modes), where $\beta = 1/k_B T$, k_B is the Boltzmann constant, T is temperature, $\hbar = h/2\pi$ is the reduced Planck constant and μ is the chemical potential. The summation can be changed to an integral with a continuous state variable and a suitable DOS: $N = \int_{\omega_0}^{\infty} \rho(\omega) d\omega/\{\exp\beta[\hbar(\omega_i - \omega_0) - \mu] - 1\}$.

The critical photon number for condensation in the cavity is given by [4]

$$N_c = \int_{\omega_0}^{\infty} \frac{s\rho(\omega)d\omega}{e^{\beta\hbar(\omega-\omega_0)} - 1} \approx \int_{\omega_0}^{\infty} \frac{sb(\omega - \omega_0)^{\alpha} d\omega}{e^{\beta\hbar(\omega-\omega_0)} - 1} + \int_{\omega_1}^{\infty} \frac{s\rho_0 d\omega}{e^{\beta\hbar(\omega-\omega_0)} - 1} \tag{4}$$
$$, = (bs/\hbar^{\alpha+1})\,\Gamma(\alpha+1)\,\zeta(\alpha+1)\,(k_B T)^{\alpha+1} + s\,x\,\ln x,$$

where $\omega_1 = \omega_0 + \pi c/nl_0$ is the next to the cutoff mode, $x = 2nl_0 k_B T/hc$ and $\Gamma(z)$ and $\zeta(z)$ are the gamma and the Riemann zeta functions. The general BE distribution is proportional to $1/(e^{\beta[\hbar(\omega-\omega_0)-\mu]} - 1)$. At BEC $\mu = 0$. BEC is possible when the integral for N_C in Eq. (4), that starts from the cutoff ω_0, converges. Then all states above the ground state are filled at a critical temperature (or a critical particle number) defined in Eq. (4) and any additional pumping (or decrease of the temperature) adds particles to the ground state. It requires that the exponent of $\rho(\varepsilon)$ is positive: $(1/\eta) - 1 > 0$ or $\eta < 1$ ($\eta > 0$). (More generally for a dimension d: $N_c \propto (k_B T)^{d/\eta}$, and the condition for BEC is $(d/\eta) - 1 > 0$, or $\eta < d$ ($\eta > 0$). For the constant part of the DOS, ρ_0, convergence is possible due to finite cavity length consideration and starting the integral from the second mode ω_1, as discussed in Ref. [4]. We also note that due to the FP transmission modes with a relatively large width, related to a low FP finesse for the continuous wavelengths of the chirped fiber Bragg gratings, we have in Eq. (4) an additional multiplying parameter s, that we discuss and quantify below. It reflects the partial dilution effect of the FP modes that each still contains many long cavity modes (except the BEC mode, as we note below). The convergence of the first integral in Eq. (4) is possible when the exponent in $\rho(\omega) \propto (\omega - \omega_0)^{\alpha}$ is positive ($\alpha > 0$), that is met in the linear chirped fiber Bragg gratings case where $\alpha = 1$. Starting the integral right at the frequency cutoff ω_0 and having convergence with such DOS makes the BEC valid in the large system limit where the cavity length $l \to \infty$ without the need of a finite cavity consideration [4]. The second integral in Eq. (4) with ρ_0 converges only for a finite system size [4,10], but as we see below, it is anyhow small for $l_0 \approx 0$ at higher than 100 K, compared to the first integral [15]. The calculation of this second term is similar to what we had for a finite system size with a linear dispersion [4], that gave a logarithmic dependence at the origin ($\varepsilon = 0$) but converges when the lower bound is taken from the second mode and not from zero, as it should be for N_c. However, as we noted above, this second term is smaller than the quadratic one. For the linear

Optics EXPRESS

chirp case ($\alpha = 1$) Eq. (4) gives:

$$N_c \approx (bs\pi^2/6\hbar^2)(k_B T)^2 + s\,x \ln x \approx 0.039\ s\,T^2 + s(200\,l_0 T)\ln(200\,l_0 T) \approx 0.039\ s\,T^2 + 1000\,l_0\,s\,T \quad (5)$$

where we used $\Gamma(2) = 1$ and $\zeta(2) = \pi^2/6$. Here the coefficients of T^2 and T have units of $1/K^2$ and $1/(K\ m)$ respectively. The second term is negligible when $l_0 << 3.9 \times 10^{-5}\,T$. For T=300 K it gives $l_0 << 11.7\,mm$ that can be implemented in the experiment. For $l_0 = 2.8\,mm$, $T >> 1000 l_0/0.039 \approx 72K$. We used an average value for $\ln(200\,l_0 T) \approx 5$. Therefore, in our experiment the T^2 term dominates above 100 K. We stress that then the BEC results is valid in the in the large cavity limit, although the number of FP modes in the chirped fiber Bragg gratings band of 32.5 nm (the maximum transmission range of the wave-shaper), was relatively small [15]: $m \sim 500$. To get a feeling of the critical power values, we have for $T = 300K$: $N_c \approx 0.433\,s \times 10^4$ photons. Converting N to power is done by $P = N\hbar\omega/t_{rt}$ where $t_{rt} = l/(c/n)$ is the whole cavity photon round-trip time. For the calculation we take the experimental length of $l \approx 27m$ and $2l_0 \approx 2 \times 2.8\,mm$. Then we have $N_0 = N - N_c \approx N - 0.039\ s\,T^2$ that gives for the condensation and critical powers, p_0 and $P_c = P(p_0 = 0)$, respectively:

$$p_0 = P - P_c = P - \tilde{a}\,T^2, \qquad P_c = \tilde{a}\,T^2 \quad (6)$$

where $\tilde{a} = 0.039\,s\hbar\omega_0\,c/nl \approx 1.23 \times 10^{-5}\mu W/K^2$ with $s = 321$. It gives, for example $P_c(T = 300K) \approx 1.1\mu W$.

3. Experiment

3.1. System

The experimental system is described in Fig. 1. It is similar to the one in Ref. [4] besides the cutoff element and a Fabry-Perot that provided sublinear mode-dispersion ($\eta = 0.5$). The FP that is placed in a long ring cavity $l = 27\,m$ with the square-root mode-dispersion dilutes the long cavity modes and determines the BEC occurrence as discussed below. The $(9 + 1)\,m$ long double-clad EYDF sections give photon gain that keeps the photon number almost constant and thermalization.

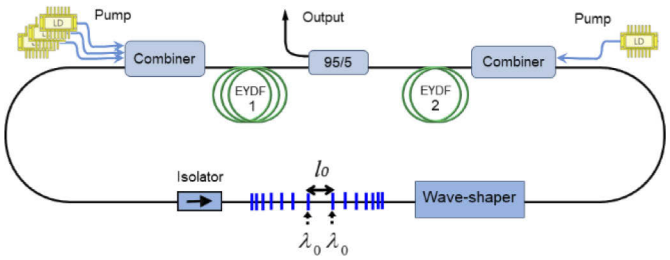

Fig. 1. The fiber cavity schematic for the photon BEC experiment: It contains the chirped fiber Bragg gratings FP, two double-clad EYDF sections for gain and thermalization and a wave-shaper that determines the spectral range including the cutoff wavelength. The counter-propagating cladding pumping was used to obtain a more uniform pump level along the entire length of the active fiber.

In the experiment, the EYDF gave the photon thermalization [4,16], and the wave-shaper (1000S of Finisar based on angular dispersion and liquid crystal on a Silicon array to form the required spectral filter) with the chirped grating FP provided the cutoff wavelength at $\lambda_0 \approx 1560.5\,nm$ (slightly lower than the wavelength of the grating's chirp edge), that are requirements for BEC. The modes of the FP filter and select the dense ring cavity modes that have

Optics EXPRESS

a spacing of $\Delta\nu_{cavity} = c/nl$. A use of the wave-shaper has advantages compared to the cutoff filter [4], mainly since its cutoff width was less than 1 *nm*, compared to 4 *nm* in the filter case. Nevertheless, the wave-shaper also added a low wavelength bound at 1528 *nm*, besides the high wavelength at 1560.7 *nm* that served as the cutoff, such that the transmission band was 32.5 *nm*. The extinction ratio was 50 *dB*, similar to the filter case. Nevertheless, the loss was higher, about 3 *dB* and it restricted the maximum upper wavelength cutoff at 1560.7 *nm*. The higher losses that sum to (70-90)% and gave a relatively long photon cavity lifetime of $t_c \sim (1-2)\times 10^{-7} s$ due to the long size of the cavity (27 *m*) still let us be in the low loss-rate "quantum" regime [12]. We used linear gratings for the Fabry-Perot ($\alpha = 1$), with a short spacing of $l_0 = 2.8$ *mm* between them. For the temperature variation and its measurement, we used the setup and the methods that were described in our former work [4].

3.2. Measurements

We show the experimental results using a Fabry-Perot with linearly chirped gratings ($\alpha = 1$) using the system shown in Fig. 1. In Fig. 2 we can see spectra for different pumping levels that give intracavity powers below and above the condensation critical power. The resolution of the spectra in Fig. 2 was 20 *pm* with averaging to increase the range of the signal level. The condensation that was at ~1560.7 *nm* occurred at a single long cavity (fiber-ring-cavity) mode (in many experiments, but not always, maybe due to noise). This can be seen in the inset of Fig. 2 done with a pumping slightly above threshold and measured with the spectrum analyzer with a high resolution of 10 *MHz* or 0.08 *pm*, while the long cavity (27 *m*) mode separation was ~7.7 *MHz*. The Bose-Einstein (BE) spectra that fit the corresponding temperatures (300 *K* in Fig. 2) reflect the photon thermalization effect [4,16]. We stress that for additional pumping beyond threshold where $\mu = 0$ the additional power goes to the mode near the cutoff. Any deviation can be due to several reasons. It can hint on a photon quasi-equilibrium or nonequilibrium near and above condensation that can be a very interesting phenomenon [5,6], and deserves a special work and paper**.** We also note that the experimental spectra without the restricting wave-shaper and the chirped gratings showed a larger range that started from 1460 *nm* below and above condensation followed BE distribution at 300 *K* for all pumping values with an almost straight line with a slope that fits the temperature (as was observed in Refs. [4,16]) with a range of 100-200 *nm*) until the effect of the cutoff and condensation caused a deviation from it. Another point is the large fluctuations above condensation [26]. There is also an effect of the low resolution spectra. The measured spectra near condensation give an average of narrow width signals and close to zero background that can be seen in the inset of Fig. 2. It causes a lower power in the measurement of the spectra in Fig. 2 except for the condensation zone at or near the cutoff. As we discussed earlier [4,16], the photon thermalization depends on interactions with the erbium atoms in the fiber core. In our system with relatively long active fibers and high doping concentration, there are many photon-erbium interaction cycles that are needed for photon thermalization [3,4,12,16].We can also see in Fig. 2 the FP modes with the nonuniform mode spacing determined by the chirped fiber Bragg gratings FP.

Figure 3 shows the critical powers for condensation for the nonuniform mode comb with a linear chirp (opposite chirp directions) and for a uniform mode comb FP (chirped gratings in the same direction) cases with a quadratic and linear fits that follow the theory. The experiment was done in a broad temperature range between 90 *K* and 382 *K*, using the measurement, cooling and heating apparatus and methods described in our former work [4]. We note that the measurement of the condensation mode power p_0 obtained with an integration of the spectra measured with YOKOGAWA AQ6370D spectrum analyzer, here is more definitive than what we had in the fiber cavity experiment in Ref. [4] since the modes defined by the FP are distinctive and can be observed by the spectrum analyzer. As the pumping increases the condensation power p_0 becomes larger than the former chirped gratings FP mode by more than 27 *dB*. We also stress that

Optics EXPRESS

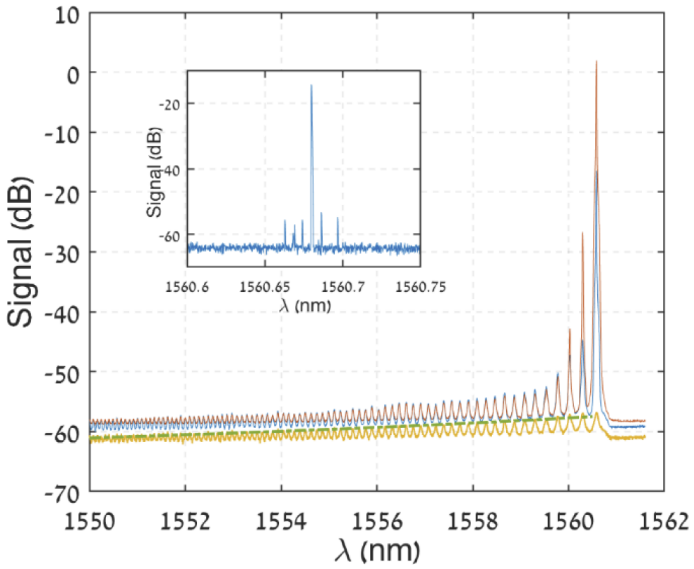

Fig. 2. The condensation experimental results. Showing spectra in arbitrary units for three pumping levels (overall powers), one below BEC threshold and two above it. Above threshold, most power goes to the condensation mode. The almost straight dark green dashed line gives a fit of the theoretical BE distribution for 300 K below the condensation threshold with a chemical potential fit of $\mu = -0.2/\beta \approx -0.0052eV$, complying with the thermal equilibrium of the photons in the cavity. For strong pumping the condensation power p_0 becomes larger than the former mode by more than 27 dB. We can see the FP modes with the nonuniform spacing determined by the chirped fiber Bragg gratings FP with $\alpha = 1$, and the condensation near the cutoff. For pumping at and above threshold $\mu = 0$**.** For further pumping above threshold $\mu = 0$ and only the condensation mode grows. We note that the experimental spectra without the wave-shaper and the chirped gratings had a larger range that started from 1460 nm followed BE distribution at 300 K for all pumping values with an almost straight line, as was observed in Refs. [4,16], until the effect of the cutoff caused a deviation from it. Here the spectra were measured by an optical spectrum analyzer with a resolution of 20 pm and averaging to obtain large dynamic range. Inset: Zoom at the lower (condensation) mode with a high resolution of 10 MHZ (0.08pm) with a pumping that is slightly above threshold. It gives for the strong line a maximum width of $\Delta\nu$<10MHz or $\Delta\lambda$<0.08pm that means very high coherence length of l_C>300 m. This line is higher by ~40 dB from the low weak secondary or noisy mode spikes.

the condensation accumulation is at a very narrow spectral width of a single long cavity mode, as can be seen in the inset of Fig. 2, measured by a spectrum analyzer with high resolution of 10 MHz (0.08 pm) (AP2041B of APEX Technologies that is based on interferometric method and includes a tunable laser as a local oscillator with a linewidth of 500 kHz) in many experiments, but not always, maybe due to noise.

The experimental measurements for the nonuniform comb shown in Fig. 3 gave $P_C = [(1.23 \pm 0.16) \times 10^{-5}T^2 + 0.22 \pm 0.08\,]\,\mu W$, that with the deduction of the constant value of $\approx 0.22\mu W$ fits the theoretical values for the critical powers with $s = 321$. We think that this small constant power of $0.22\mu W$ results from the low temperature contribution of the second term in Eq. (5), and also from polarization reasons. As said in the theoretical part the factor s results from the relatively low FP finesse of ~4, where each of its modes still contains many long cavity modes. Nevertheless, at the condensation wavelength near the cutoff wavelength we found only a single mode, as seen in the inset of Fig. 2, (as said above, in many

Optics EXPRESS

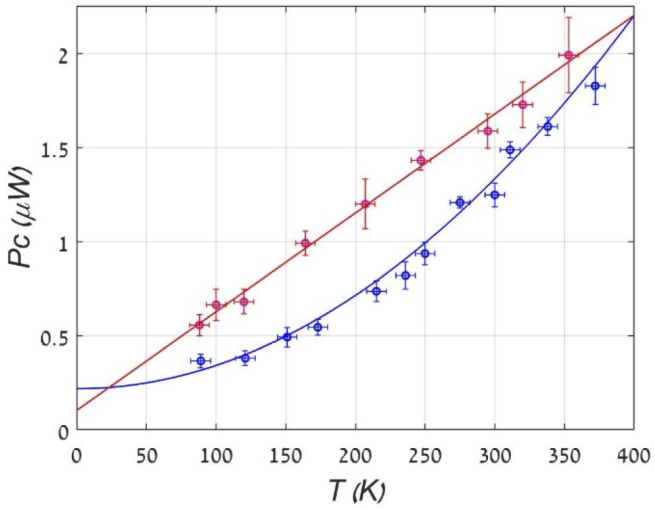

Fig. 3. The condensation critical power dependence on temperature. For the linear chirped fiber Bragg gratings case ($\alpha = 1$) that gives a square-root mode-dispersion, the experimental results gave a quadratic dependence on T (the blue points and line), $P_c = \tilde{a}_{\exp} T^2$ with $\tilde{a}_{\exp} \approx 1.23{\times}10^{-5} \mu W/K^2$ that fits the theory. For comparison, we also show the experimental results placing in the cavity a FP with a uniform comb (the chirp had the same direction in the two gratings, thus the FP separation was independent on wavelength). In this case we obtained a linear T dependence (the red points and line), as shown in the figure. The results follow the theoretical predictions. It is similar to the linear dispersion case (Ref. 4) where BEC is based on a finite cavity effect. For the temperature variation we used, as done in Ref. 4, a heating chamber with a controlled temperature that was measured by a thermocouple and a temperature dependent resistor. For cooling, we used a cryostat system with liquid nitrogen in a dry dewar where the EYDF was placed in different heights to have various temperatures.

experiments, but not always), within the spectrum analyzer resolution of $10\,MHz$ ($0.08\ pm$). For example, the value $P_c(T = 300K) \approx 1.3 - 0.22 \approx 1.08\,\mu W$ fits the theoretical calculation of $P_c = \tilde{a}\,T^2 = 1.23 \times 10^{-5} \times 300^2 = 1.1\,\mu W$. Also the experimental quadratic T dependence coefficient in Fig. 3 is $\tilde{a}_{\exp} \approx (1.23 \pm 0.16) \times 10^{-5} \mu W/K^2$, that excellently agrees with the theoretical value of $\tilde{a} \approx 0.383\,s \times 10^{-7} \mu W/K^2 = 1.23 \times 10^{-5} \mu W/K^2$, for a linear chirp with the same $s = 321$.

For comparison, we also made measurements for a FP that we fabricated with two gratings that have the same chirp direction that was placed it in the long EYDF cavity. Such FP gave the same "mirror" separation of $l_{FP} \approx 2.13\,mm$ for all wavelengths and therefore generated a regular uniform mode comb separation and a linear dispersion at a large band of ~45 nm. (We note that the gratings here partially overlapped and the spacing between the same wavelength locations in the two gratings that gives the FP width was $l_{FP} \approx 2.13\,mm$ for all wavelengths.) Then $b = 0$ and we have a constant DOS: $\rho(\omega) = \rho_0 = nl_{FP}/\pi c$ which is on the boundary for BEC formation. It provided condensation, as we had in Ref. [4], but it relied on finite cavity size effect. It theoretically gives a linear P_C dependence on T, $P_c = (\hbar\omega_0/t_{rt})s' x \ln x \approx aT$, where $x = 2n\,l_{FP}\,k_B T/hc$ and a $\approx$ s' $1.13 \times 10^{-5} \mu$W/K. We used $l_{FP} \approx 2.13\,mm$ and an average value for the factor ln x ≈ 4.36, that doesn't vary much in the relevant temperature range. Here we had a different factor s' and understandably larger than the former s due to larger mode spacing ($\Delta\upsilon \approx 50\,Ghz$) and only $m \sim 81$ FP modes in the $32.5\,nm$ band case compared to the smaller average spacing in the opposite chirp direction case. The experimental dependence of $P_C(T)$ for this FP, shown in Fig. 3

Optics EXPRESS

indeed gave a linear dependence on T, $P_C = [(5.38 \pm 0.5) \times 10^{-3}\, T + 0.086 \pm 0.01\,]\mu W$ with a slope $a_{\exp} \approx 5.38 \times 10^{-3}\,\mu W/K$ that with $s' = 2952$ gave a good agreement with the theory. For example, the critical power value at $300\,K$ is $P_c(T = 300K) = aT \approx 1.6\,\mu W$. Altogether, these measurements furtherly support the condensation observation.

4. Summary

We have demonstrated condensation of photons in a fiber cavity by using a special method for obtaining sublinear mode-dispersion required for BEC in the large cavity limit. It was done in the experiment by adding a linearly chirped-gratings FP in the cavity that gave a square-root mode-dispersion relation [15]. We demonstrated condensation and a quadratic temperature dependence of the critical power for condensation that followed the theoretical prediction for condensation with a square-root mode-dispersion. It is different from the linear temperature dependence in cavities with regular fibers that have a linear or close to linear dispersion where the BEC relies on the finite size effect [4]. These findings, besides the thermal spectra and the near cutoff population, support the condensation observation.

Funding. Israel Science Foundation.

Disclosures. The authors declare no conflicts of interest.

Data availability. Data underlying the results presented in this paper are not publicly available at this time but may be obtained from the authors upon reasonable request.

References

1. M. H. Anderson, J.R. Ensher, M.R. Matthews, C. E. Weiman, and E. A. Cornell, "Observation of Bose-Einstein condensation in a dilute atomic vapor," Science **269**(5221), 198–201 (1995).
2. K. D. Davis, M. O. Mewes, M. R. Andrews, N. J. vanDruten, D. S. Durfee, D. M. Kurn, and W. Ketterle, "Bose-Einstein condensation in a gas of sodium atoms," Phys. Rev. Lett. **75**(22), 3969–3973 (1995).
3. J. Klaers, J. Schmitt, F. Vewinger, and M. Weitz, "Bose-Einstein condensation of photons in an optical microcavity," Nature **468**(7323), 545–548 (2010).
4. R. Weill, A. Bekker, B. Levit, and B. Fischer, "Bose-Einstein condensation of photons in an Erbium Ytterbium co-doped fiber cavity," Nature Comm. **10**(1), 747 (2019).
5. H. Deng, G. Weihs, C. Santori, J. Bloch, and Y. Yamamoto, "Condensation of semiconductor microcavity exciton polaritons," Science **298**(5591), 199–202 (2002).
6. J. Kasprzak, M. Richard, S. Kundermann, A. Baas, P. Jeambrun, J.M.J. Keeling, F.M. Marchetti, M.H. Szymańska, R. André, J.L. Staehli, and V. Savona, "Bose–Einstein condensation of exciton polaritons," Nature **443**(7110), 409–414 (2006).
7. Y. Sun, P. Wen, Y. Yoon, G. Liu, M. Steger, L. N. Pfeiffer, K. West, D. W. Snoke, and K. A. Nelson, "Bose-Einstein Condensation of Long-Lifetime Polaritons in Thermal Equilibrium," Phys. Rev. Lett. **118**(1), 016602 (2017).
8. S. O. Demokritov, V. E. Demidov, O. Dzyapko, G. A. Melkov, A. A. Serga, B. Hillebrands, and A. N. Slavin, "Bose-Einstein condensation of quasi-equilibrium magnons at room temperature under pumping," Nature **443**, 430 (2006).
9. V. Bagnato and D. Kleppner, "Bose-Einstein condensation in low-dimensional traps," Phys. Rev. A. **44**(11), 7439–7441 (1991).
10. W. Ketterle and N. J. van Druten, "Bose-Einstein condensation of a finite number of particles trapped in one or *three* dimensions," Phys. Rev. A **54**(1), 656–660 (1996).
11. J. Marelic and R. A. Nyman, "Experimental evidence for inhomogeneous pumping and energy-dependent effects in photon Bose-Einstein condensation," Phys. Rev. A **91**(3), 033813 (2015).
12. J. Klaers, F. Vewinger, and M. Weitz, "Thermalization of a two-dimensional photonic gas in a white wall photon box," Nat. Phys. **6**(7), 512–515 (2010).
13. J. Schmitt, T. Damm, D. Dung, F. Vewinger, J. Klaers, and M. Weitz, "Thermalization kinetics of light: From laser dynamics to equilibrium condensation of photons," Phys. Rev. A **92**(1), 011602 (2015).
14. S. Barland, P. Azam, G. L. Lippi, R. A. Nyman, and R. Kaiser, "Photon thermalization and a condensation phase transition in an electrically pumped semiconductor microresonator," Opt. Express **29**(6), 8368 (2021).
15. A. Bekker, B. Levit, R. Weill, and B. Fischer, "Nonlinear light mode-dispersion and nonuniform mode comb by a Fabry-Perot with chirped fiber gratings," Opt. Express **28**(12), 18135 (2020).
16. R. Weill, A. Bekker, B. Levit, M. Zhurahov, and B. Fischer, "Thermalization of one-dimensional photon gas and thermal lasers in erbium-doped fibers," Opt. Express **25**(16), 18963 (2017).
17. P. Kirton and J. Keeling, "Thermalization and breakdown of thermalization in photon condensates," Phys. Rev. A **91**(3), 033826 (2015).

Optics EXPRESS

18. I. Carusotto and C. Ciuti, "Quantum fluids of light," Quantum fluids of light," Rev. Mod. Phys. **85**(1), 299–366 (2013).
19. A. Picozzi, J. Garnier, T. Hansson, P. Suret, and S. Randoux, "Optical wave turbulence: Towards a unified nonequilibrium thermodynamic formulation of statistical nonlinear optics," Physical Reports **542**(1), 1–132 (2014).
20. C. Sun, S. Jia, C. Barsi, S. Rica, A. Picozzi, and J. W. Fleischer, "Observation of the kinetic condensation of classical waves," *Nat. Phys*. **8**(6), 470–474 (2012).
21. K. Baudin, A. Fusaro, K. Krupa, J. Garnier, S. Rica, G. Millot, and A. Picozzi, "Classical Rayleigh-Jeans Condensation of Light Waves: Observation and Thermodynamic Characterization," Phys. Rev. Lett. **125**(24), 244101 (2020).
22. B. Fischer and R. Weill, "When does single-mode lasing become a condensation phenomenon?" Opt. Express **20**(24), 26704 (2012).
23. R. Weill, B. Fischer, and O. Gat, "Light-mode condensation in actively mode-locked lasers," Phys. Rev. Lett. **104**(17), 173901 (2010).
24. G. Oren, A. Bekker, B. Levit, R. Weill, and B. Fischer, "Classical condensation of light pulses in a loss trap in a laser cavity," Optica **1**(3), 145 (2014).
25. M. Zhurahov, A. Bekker, B. Levit, R. Weill, and B. Fischer, "CW laser light condensation," Opt. Express **24**(6), 6553 (2016).
26. W. J. Mullin and J. P. Fernandez, "Bose-Einstein condensation, fluctuations, and recurrence relations in statistical mechanics," Am. J. Phys. **71**(7), 661–669 (2003).